

AD-A102 114

ARMY COMMUNICATIONS-ELECTRONICS ENGINEERING INSTALLAT--ETC F/G 17/2,1  
ESTIMATED PERFORMANCE OF A QPRS RADIO IN THE PRESENCE OF FREQUE--ETC(U)

JUN 81 S T MATSUURA  
UNCLASSIFIED CCC-EMEO-PED-81-8

NL

1 OF 1  
ADA  
02114

END  
DATE  
FILED  
9-81  
DTIC

(3)



Electromagnetics Engineering Office  
Propagation Engineering Division  
Technical Report EMEO-PED-81-8

LEVEL II

ADA102114

ESTIMATED PERFORMANCE OF A QPRS  
RADIO IN THE PRESENCE OF FREQUENCY  
SELECTIVE FADING

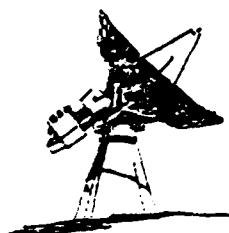
DTIC  
ELECTE  
S JUL 27 1981 D  
E

By

Stephen T. Matsuura

June 1981

DTIC FILE COPY



DISTRIBUTION STATEMENT:

Approved for public release;  
distribution unlimited.

HEADQUARTERS  
US ARMY COMMUNICATIONS-ELECTRONICS  
ENGINEERING INSTALLATION AGENCY  
Fort Huachuca, Arizona 85613

817 27 179

DEPARTMENT OF THE ARMY  
US ARMY COMMUNICATIONS-ELECTRONICS  
ENGINEERING INSTALLATION AGENCY  
Fort Huachuca, Arizona 85613

This Technical Report was prepared by the Propagation Engineering Division, Electromagnetics Engineering Office, of the Communications-Electronics Engineering Installation Agency and is published for the information and guidance of all addressees. Suggestions and criticism relative to the form, contents, purpose, or use of this publication should be referred to the attention of the Commander, US Army Communications-Electronics Engineering Installation Agency, ATTN: CCC-EMEO-PED, Fort Huachuca, Arizona 85613. Technical comments may be coordinated directly with the author, at (602) 538-6779 or AUTOVON 879-6779.

MILES A. MERKEL  
Chief, Electromagnetics Engineering Office

Accession For	
NTIS GRA&I	<input checked="" type="checkbox"/>
DTIC TAB	<input type="checkbox"/>
Unannounced	<input type="checkbox"/>
Justification	
By _____	
Distribution/	
Availability Codes	
Distr	Avail and/or Special
A	

DISPOSITION

Destroy this report when it is no longer needed.  
Do not return it to the originator.

## UNCLASSIFIED

SECURITY CLASSIFICATION OF THIS PAGE (When Data Entered)

REPORT DOCUMENTATION PAGE		READ INSTRUCTIONS BEFORE COMPLETING FORM
1. REPORT NUMBER <i>EMEO-PED-81-8</i>	2. GOVT ACCESSION NO. <i>(Q) AD-A101 214</i>	3. RECIPIENT'S CATALOG NUMBER
4. TITLE (and Subtitle) <b>ESTIMATED PERFORMANCE OF A QPRS RADIO IN THE PRESENCE OF FREQUENCY SELECTIVE FADING</b>	5. TYPE OF REPORT & PERIOD COVERED <i>Final Report</i>	
7. AUTHOR(s) <i>Stephen T. Matsuura</i>	8. CONTRACT OR GRANT NUMBER(s)	
9. PERFORMING ORGANIZATION NAME AND ADDRESS USACEEIA ATTN: CCC-EMEO-PED Fort Huachuca, Arizona 85613	10. PROGRAM ELEMENT, PROJECT, TASK AREA & WORK UNIT NUMBERS	
11. CONTROLLING OFFICE NAME AND ADDRESS USACEEIA ATTN: CCC-EMEO-PED Fort Huachuca, Arizona 85613	12. REPORT DATE <i>June 1981</i>	
14. MONITORING AGENCY NAME & ADDRESS (if different from Controlling Office)	13. NUMBER OF PAGES <i>13 48</i>	
	15. SECURITY CLASS. (of this report) <b>UNCLASSIFIED</b>	
	15a. DECLASSIFICATION/DOWNGRADING SCHEDULE	
16. DISTRIBUTION STATEMENT (of this Report) <b>Approved for public release; distribution unlimited</b>		
17. DISTRIBUTION STATEMENT (of the abstract entered in Block 20, if different from Report)		
18. SUPPLEMENTARY NOTES		
19. KEY WORDS (Continue on reverse side if necessary and identify by block number) <b>Digital LOS Radio, QPRS Radio, Multipath, Frequency Selective Fading</b>		
20. ABSTRACT (Continue on reverse side if necessary and identify by block number)		
<ol style="list-style-type: none"> <li>1. This report provides an estimation of the probability of outage of a QPRS radio (Aventek DR-8A) link in a multipath caused frequency selective fading environment.</li> <li>2. This performance estimation is based on:           <ol style="list-style-type: none"> <li>a propagation channel model with transfer function of the form <math>H(w) = a(1+b \exp[-j(wt+\phi)])</math>, which has been derived from experimental data.</li> <li>b. A laboratory simulation of the model with DR-8A radios to determine</li> </ol> </li> </ol>		

UNCLASSIFIED

SECURITY CLASSIFICATION OF THIS PAGE(When Data Entered)

20.

the range of values of the channel model parameters that degrade radio performance.

c. Assumed probability density functions for the channel model parameters (as random variables), based on sparse experimental data.

3. The experimental data shows that:

a. Radio performance degradation begins (above the flat fade case) with delays ( $\tau$  in the transfer function) in the order of a few nanoseconds.

b. Longer delays cause increased degradation.

c. For degradation to occur, the function minimum must occur within a few megahertz of the radio passband.

4. The estimated probability of the fade outage (based on measured parameters of the DR-8A radio), indicate that:

a. The predicted outage for distances greater than 25 miles is higher than that predicted using flat fade methods.

b. Space diversity alone may not provide sufficient performance improvement at distances must beyond 30 miles, although the combination of space diversity and adaptive equalizer should be adequate for nearly all line-of-sight paths.

UNCLASSIFIED

SECURITY CLASSIFICATION OF THIS PAGE(When Data Entered)

ACKNOWLEDGEMENT

The experimental data used in this study was provided by the  
US Army Electronic Proving Ground, Mr. Gail Query, Test Officer.

## EXECUTIVE SUMMARY

1. This report provides an estimation of the probability of outage of a QPRS radio (Avantek DR-8A) link in a multipath caused frequency selective fading environment.
2. This performance estimation is based on:
  - a. A propagation channel model with transfer function of the form  $H(\omega) = a[1+b \exp \{-j(\omega\tau+\phi)\}]$ , which has been derived from experimental data.
  - b. A laboratory simulation of the model with DR-8A radios to determine the range of values of the channel model parameters that degrade radio performance.
  - c. Assumed probability density functions for the channel model parameters (as random variables), based on sparse experimental data.
3. The experimental data shows that:
  - a. Radio performance degradation begins (above the flat fade case) with delays ( $\tau$  in the transfer function) in the order of a few nanoseconds.
  - b. Longer delays cause increased degradation.
  - c. For degradation to occur, the function minimum must occur within a few megahertz of the radio passband.
4. The estimated probability of fade outage (based on measured parameters of the DR-8A radio), indicate that:
  - a. The predicted outage for distances greater than 25 miles is higher than that predicted using flat fade methods.

b. Space diversity alone may not provide sufficient performance improvement at distances much beyond 30 miles, although the combination of space diversity and adaptive equalizer should be adequate for nearly all line-of-sight paths.

5. It is recommended that:

- a. A follow-on study be conducted on the AN/FRC-171.
- b. The statistics for the channel model parameters be experimentally obtained.
- c. The AN/FRC-171 be tested on a link with high multipath occurrence such as the Pacific Missile Test Center.

## TABLE OF CONTENTS

<u>PARAGRAPH</u>	<u>TITLE</u>	<u>PAGE</u>
	ACKNOWLEDGEMENT .....	i
	EXECUTIVE SUMMARY .....	ii
	LIST OF TABLES AND FIGURES.....	vi
1.	INTRODUCTION .....	1
1.1	Background.....	1
1.2	General Objectives .....	1
2.	INSTRUMENTATION AND PROCEDURE .....	1
2.1	Channel Model .....	1
2.2	Laboratory Test Arrangement.....	2
2.2.1	Test Radio.....	6
2.2.2	IF Fade Simulator .....	6
2.3	Measurement Procedure.....	10
3.	RESULTS .....	12
3.1	Qualitative .....	12
3.1.1	Eye Pattern Closure.....	12
3.2	Quantitative .....	16
3.2.1	Data Obtained.....	16
3.2.2	Received Signal Level Indication.....	16
3.2.3	Critical Regions .....	22
3.3	Outage Estimation .....	22

## TABLE OF CONTENTS (cont'd)

<u>PARAGRAPH</u>	<u>TITLE</u>	<u>PAGE</u>
3.3.1	Determination of the Probability of Multipath Outage .....	22
3.3.2	Determination of Jakes' k Factor.....	29
3.3.3	Diversity Improvement.....	31
3.3.4	Media Unavailability Criterion.....	33
4.	CONCLUSIONS .....	33
5.	RECOMMENDATIONS .....	35
	REFERENCES .....	36
	APPENDIX.....	38

LIST OF TABLES AND FIGURES

<u>TABLE</u>	<u>TITLE</u>	<u>PAGE</u>
1	List of Major Equipment .....	5
2	Avatek DR-8A .....	6
3	Channel Simulator Parameter Range .....	6
4	Components for IF Fade Simulator .....	8
5		16

<u>FIGURE</u>	
1 .....	3
2 .....	4
3 .....	7
4 .....	11
5a .....	13
5b .....	13
6a .....	14
6b .....	14
7a .....	15
7b .....	15
8 .....	17
9 .....	18
10 .....	19
11 .....	20
12 .....	21
13 .....	23
14 .....	24
15 .....	25
16 .....	26
17 .....	30
18 .....	32
19 .....	34

## 1. INTRODUCTION

1.1 Background. There is evidence that digital radios are adversely affected by frequency selective fading caused by multipath propagation [1], [2], [3]. The military is in the process of acquiring a standard digital radio in the Digital Radio and Multiplexer Acquisition (DRAMA) program. This radio (AN/FRC-171) will be using quaternary phase shift keying (QPSK) and quadrature partial response signaling (QPRS) modulation techniques. While there have been studies on the effects of frequency selective fading on the digital radio, most of the data are for 8PSK which although helpful, must be extrapolated to apply to QPRS.

1.2 General Objectives. The general objective of this study was to determine whether selective fading will pose a potential problem for the AN/FRC-171 radio. To do this, this study obtained data on the effects of frequency selective fading on a QPRS radio. A simple three-ray (which can be reduced to a two-ray model) propagation channel model was simulated in the laboratory and the performance of the radio recorded under various simulated channel conditions. Additionally, the results were applied to a prediction technique so that the expected performance of this radio can be compared to others.

## 2. INSTRUMENTATION AND PROCEDURE

2.1 Channel Model. Rummel [1] has found that the propagation channel is best modeled with a simple three-ray channel model that has complex voltage transfer function of the form:

$$H(\omega) = a \{ 1 + b \exp[-j(\omega\tau + \phi)] \} \quad (1)$$

Where:

a = amplitude scaling factor for the vector sum of the direct (or first) and second rays.

b = amplitude ratio between the third ray and the vector sum of the first and second rays.

$\phi$  = arbitrary phase ( $0 \leq \phi \leq 2\pi$ )

$\tau$  = time delay

$\omega$  = radian frequency

Figure 1 is a plot of  $H(\omega)$ . This model has been simulated in the laboratory and radio performance prediction compared with observed performance [3].

2.2 Laboratory Test Arrangement. A block diagram of the laboratory test arrangement used is shown in Figure 2. The blocks inclosed by dashes are part of the test radios. Error counts from the error detector were recorded by the desk top computer which was also used to start and stop the error detector. The oscilloscope monitored the three level signal "eye" pattern and the spectrum analyzer monitored the IF spectrum. Both of these data were photographically recorded for a qualitative description of signal degradation. The frequency synthesizer was used to control the output data rate of the data generator. The variable attenuator was used to control the received signal level (RSL), and the network analyzer was used to determine the amplitude and phase of the signal as it was processed by the fade simulator. Table 1 lists the specific items used in this test.

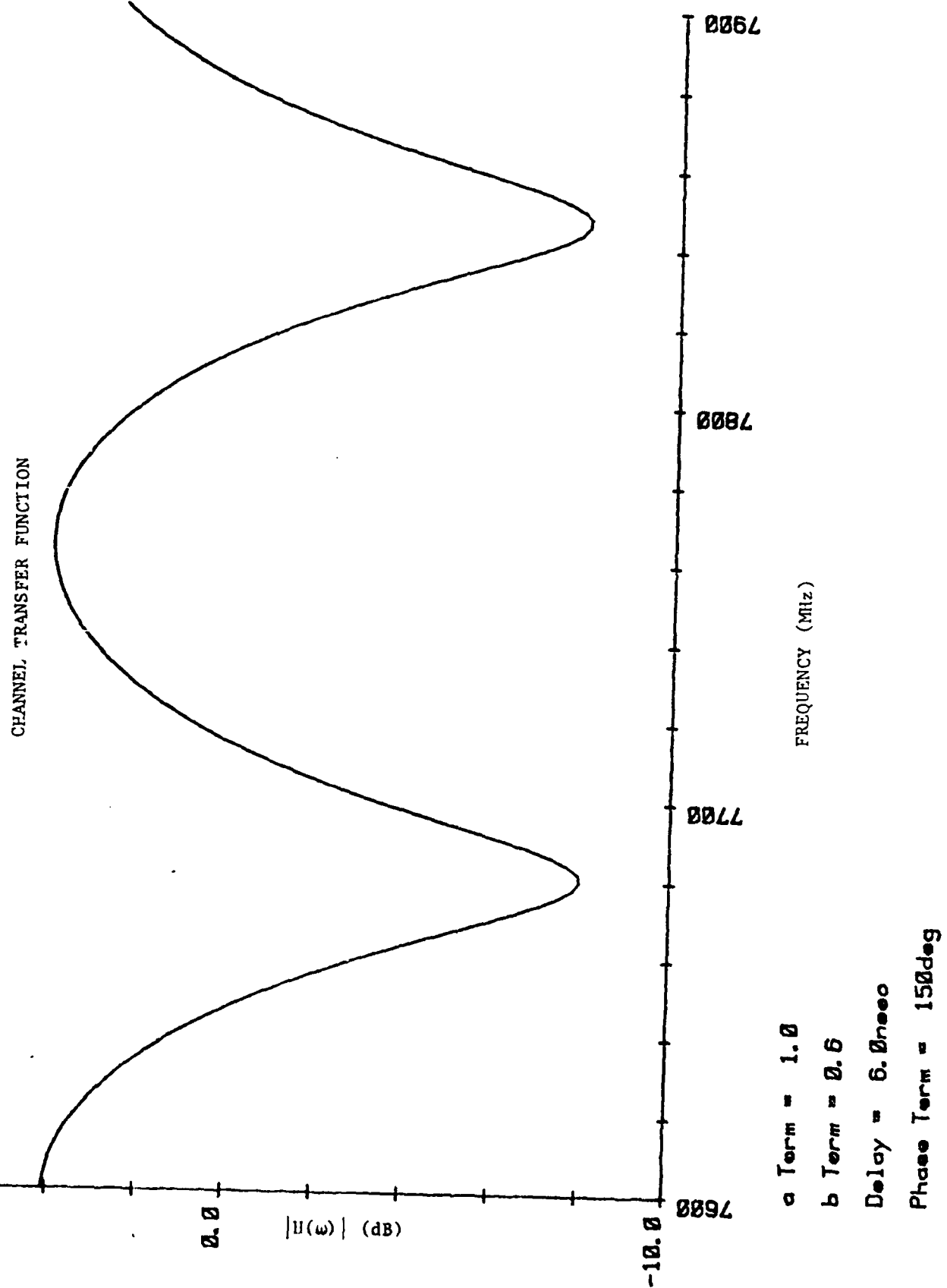
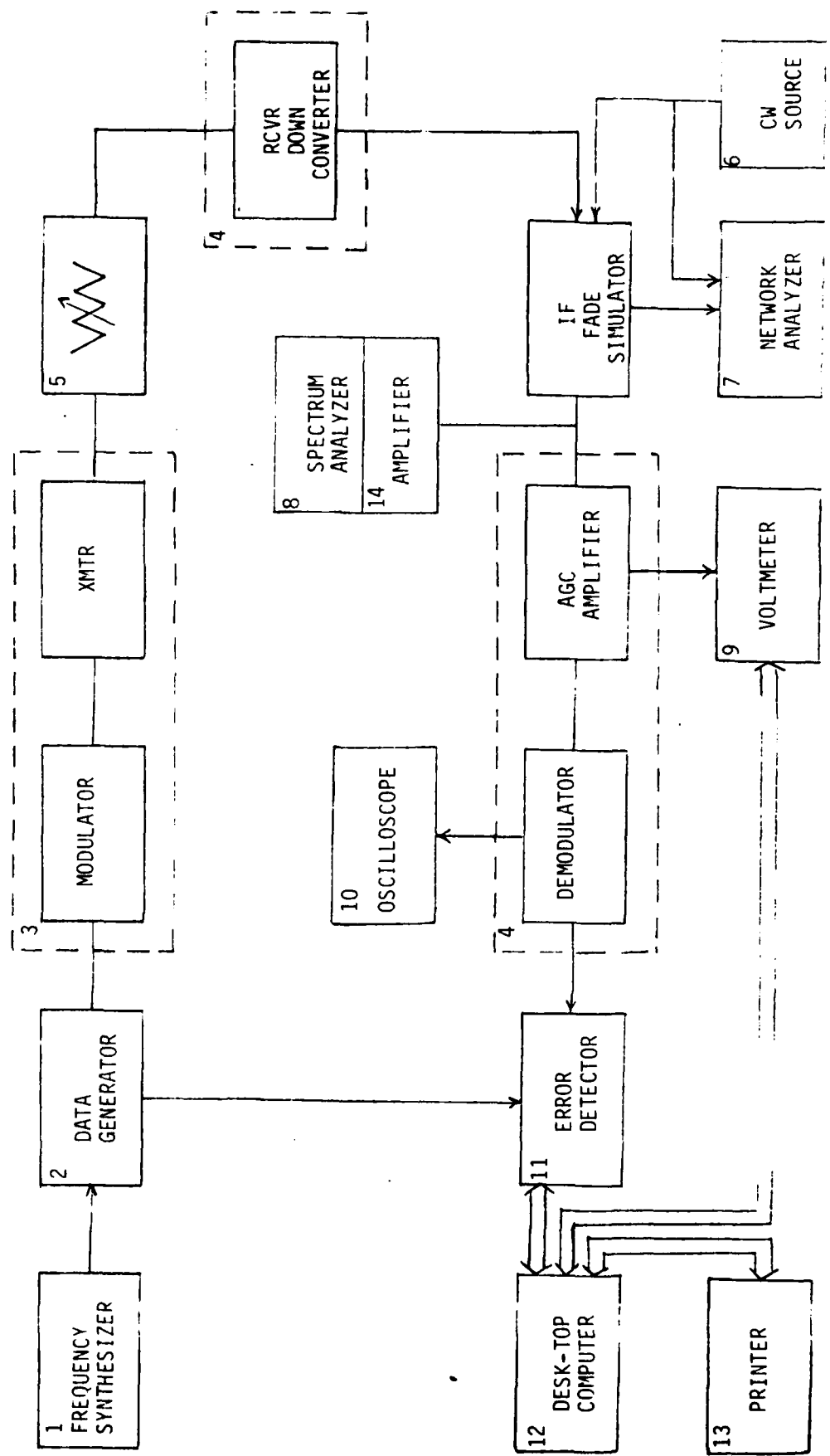


FIGURE 1



LABORATORY TEST ARRANGEMENT

FIGURE 2

TABLE 1  
List of Major Equipment

<u>Item Number</u>	<u>Item</u>	<u>Model Number</u>
1	Frequency Synthesizer	Hewlett-Packard 3320B
2	Data Generator	Hewlett-Packard 3762A
3&4	Microwave Radio	Avantek DR-8A (2)
5	Waveguide Attenuator	Waveline 506-10 506-20 506-40 Hewlett-Packard 382A
6	Signal Generator/Sweeper	Hewlett-Packard 8601A
7	Network Analyzer	Hewlett-Packard 8407A
	Phase-Magnitude Display	Hewlett-Packard 8412A
8	Spectrum Analyzer-Display Unit	Hewlett-Packard 141T
	RF Section	Hewlett-Packard 8553B
	IF Section	Hewlett-Packard 8552B
9	Digital Multimeter	Hewlett-Packard 3438A
10	Oscilloscope	Tektronix 7704A
11	Error Detector	Hewlett-Packard 3763A
12	Desktop Computer	Hewlett-Packard 9825A
	Multiprogrammer/HP1B Interface	Hewlett-Packard 59500A
	Multiprogrammer	Hewlett-Packard 6940B
	Timing Generator	Hewlett-Packard 59308A
	BCD Interface	Hewlett-Packard 98033A
13	Line Printer	Hewlett-Packard 2607A
14	Amplifier	Watkins-Johnson 6200-357/SPI

**2.2.1 Test Radio:** The Avantek DR-8A radio was used in this experiment. Table 2 provides the pertinent technical information. The Avantek DR-8A has been used as a prototype in the DRAMA program and therefore is considered to be very similar to the AN/FRC-171.

TABLE 2

Avantek DR-8A

Transmitter Power	2 watts
Transmission Rate	12.5526 Mbits/sec
Emission Bandwidth	7 MHz
Modulation Type	Three-level QPR for PCM
IF	70 MHz
Receiver Noise Figure	10 dB
Receiver IF Bandwidth	10 MHz
RSL for $10^{-6}$ BER	-74 dBm

**2.2.2 IF Fade Simulator:** Figure 3 is a block diagram of the IF fade simulator, Table 3 shows the capability (parameter range), and Table 4 lists the specific items used in the fade simulator.

TABLE 3

Channel Simulator Parameter Range

Phase ( $\phi$ )	0 to $\pm\pi$
Notch depth [20 log (1-b)]	0 to $\approx 60$ dB
Time delay ( $\tau$ )	0 to $\approx 40$ nsec

NOTE: The amplitude scaling factor  $a$  is controlled by the variable RF attenuator which is external to the IF fade simulator.

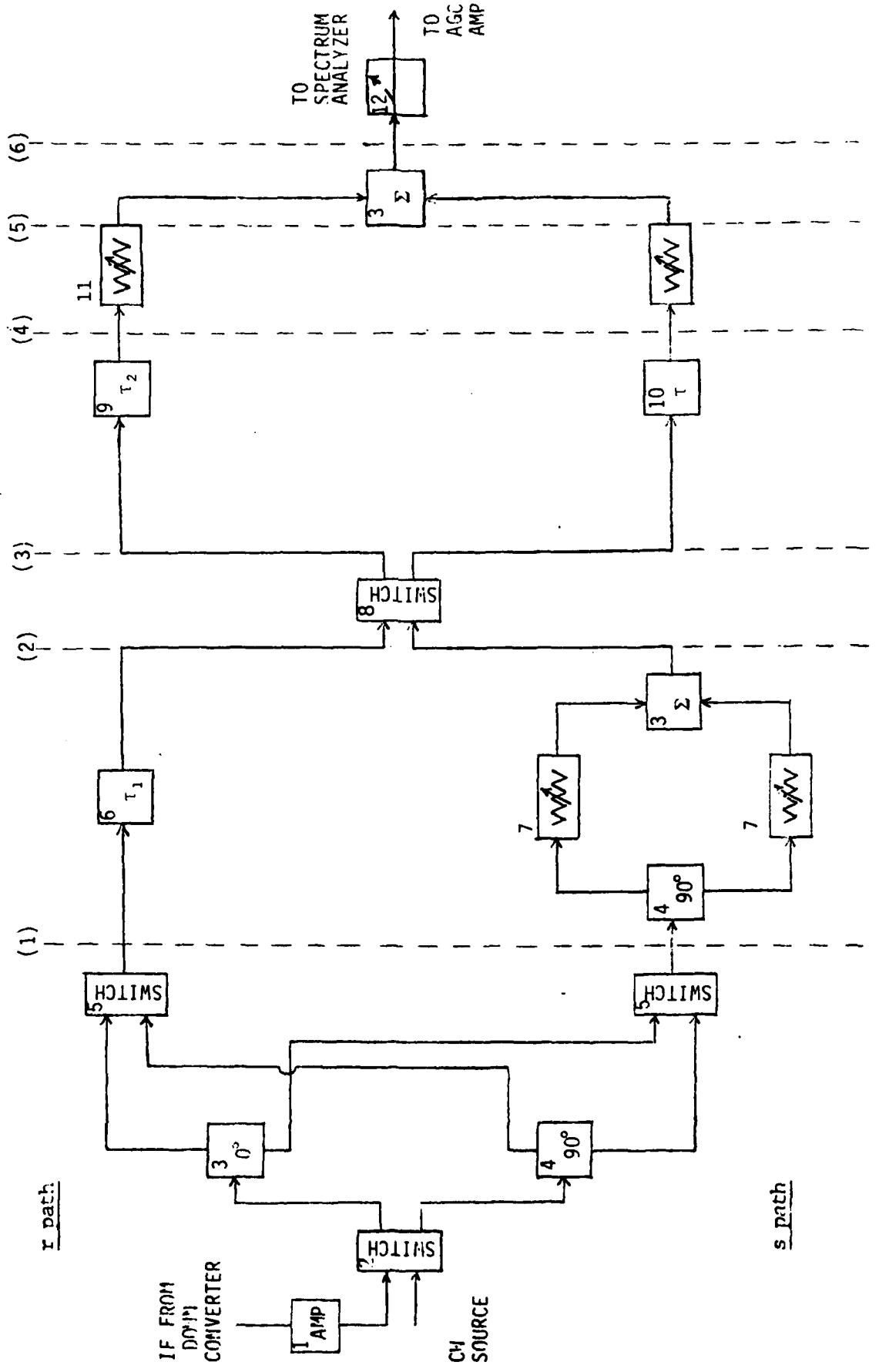


TABLE 4  
Components for IF Fade Simulator

<u>Item Number</u>	<u>Item</u>	<u>Model Number</u>
1	Amplifier	Hewlett-Packard 8447F
2	Coax Switch (2)	Amphenal 318-10381
		Amphenal 322-11421
3	Power Divider/Summer	Anzac THV-50
4	Quadrature Hybrid	Anzac JH-131
5	Coax Switch	Amphenal 322-11421
6	Variable Delay Line	Universal Ad-Yu 20B3
7	Variable Attenuator (2)	Wavetek 5080.1
		Arra 0682-10F
8	Coax Switch (4)	Hewlett-Packard 8761B
9	Delay Line (Coax Cable)	RG-58
10	Variable Delay Line	Universal Ad-Yu 20B1
11	Variable Attenuator	Alan 501L31.5
12	Directional Coupler	Wideband Engineering A73-20P

The IF signal, upon entering the fade simulator goes through a switch which selects either a 90° divider or an in-phase divider. The resultant signals at point 1 (using the top path as reference) are:

$$G_{r_1}(\omega) = F(\omega) \quad \text{where } \theta_1 = -\pi/2$$

$$G_{s_1}(\omega) = F(\omega)\exp(-j\theta_k) \quad \theta_2 = 0$$

The s path signal then goes through a 0 to 90° variable phase shifting network. There is an inherent time delay  $\tau_1$  in the variable phase shifting network. To balance this, the reference path is also delayed by  $\tau_1$  by a delay line. There is also a 90° phase shift which made it necessary to set  $\theta_1$  to -90°. The signals at point 2 are:

$$G_{r_2}(\omega) = F(\omega)$$

$$G_{s_2}(\omega) = F(\omega)\exp(-j\phi) \text{ where } 0 < \phi < \pi$$

The switch between points 2 and 3 allows either the s or r signal to be delayed. Therefore, at 3 the signals are:

$$G_{r_3}(\omega) = F(\omega)$$

$$G_{s_3}(\omega) = F(\omega)\exp(\pm j\phi)$$

The delay lines between points 3 and 4 result in:

$$G_{r_4}(\omega) = F(\omega)$$

$$G_{s_4}(\omega) = F(\omega)\exp[\pm j(\omega\tau \pm \phi)]$$

The attenuators between 4 and 5 result in:

$$G_{r_5}(\omega) = F(\omega)$$

$$G_{s_5}(\omega) = F(\omega)b\exp[\pm j(\omega\tau \pm \phi)]$$

After combining, the spectrum analyzer monitoring point 6 should see:

$$G_6(\omega) = G_{r_5}(\omega) + G_{s_5}(\omega) = F(\omega)\{1 + b\exp[\pm j(\omega\tau\phi)]\}$$

A bit error rate (BER) versus received signal level (RSL) curve for the test radios, both with and without the simulator in the circuit, is shown in Figure 4. It can be seen that the radio's performance is not disturbed by the simulator in the IF path, and also that the radio's performance is within specifications (BER less than  $10^{-6}$  for RSL of -74 dBm). See the appendix for a derivation of the equivalent IF channel transfer function.

**2.3 Measurement Procedure.** Lundgren [4] and Emshwiller [5] suggest methodologies for determining the critical values of the parameters in the channel transfer function. Reference [4] as well as [1] and [3] fixed the delay time at 6.3 nsec. Reference [5], varied time delay, but did not include the phase term ( $\Phi$ ) and the amplitude scaling term (a) as parameters in the model. In this study, all four parameters a, b,  $\tau$ ,  $\Phi$  were varied in determining the regions for outage ( $BER \geq 10^{-4}$ ).

There are many combinations in which four parameters of the transfer function can be varied with respect to each other. After trying several approaches the following procedure was used:

- a. The delay line ( $\tau$ ) is adjusted to provide the desired delay.
- b. The RF attenuator is adjusted so that the desired RSL, as indicated by the AGC voltage, is provided to the receiver front end.
- c. The desired notch frequency (location of the minimum in Figure 1) is achieved by proper selection of either 0 or 90° initial phase shift, by adjusting the attenuators in the 0-90° phase shifter and by proper routing of the signals through the switch between points (2) and (3), (SEE FIGURE 3).

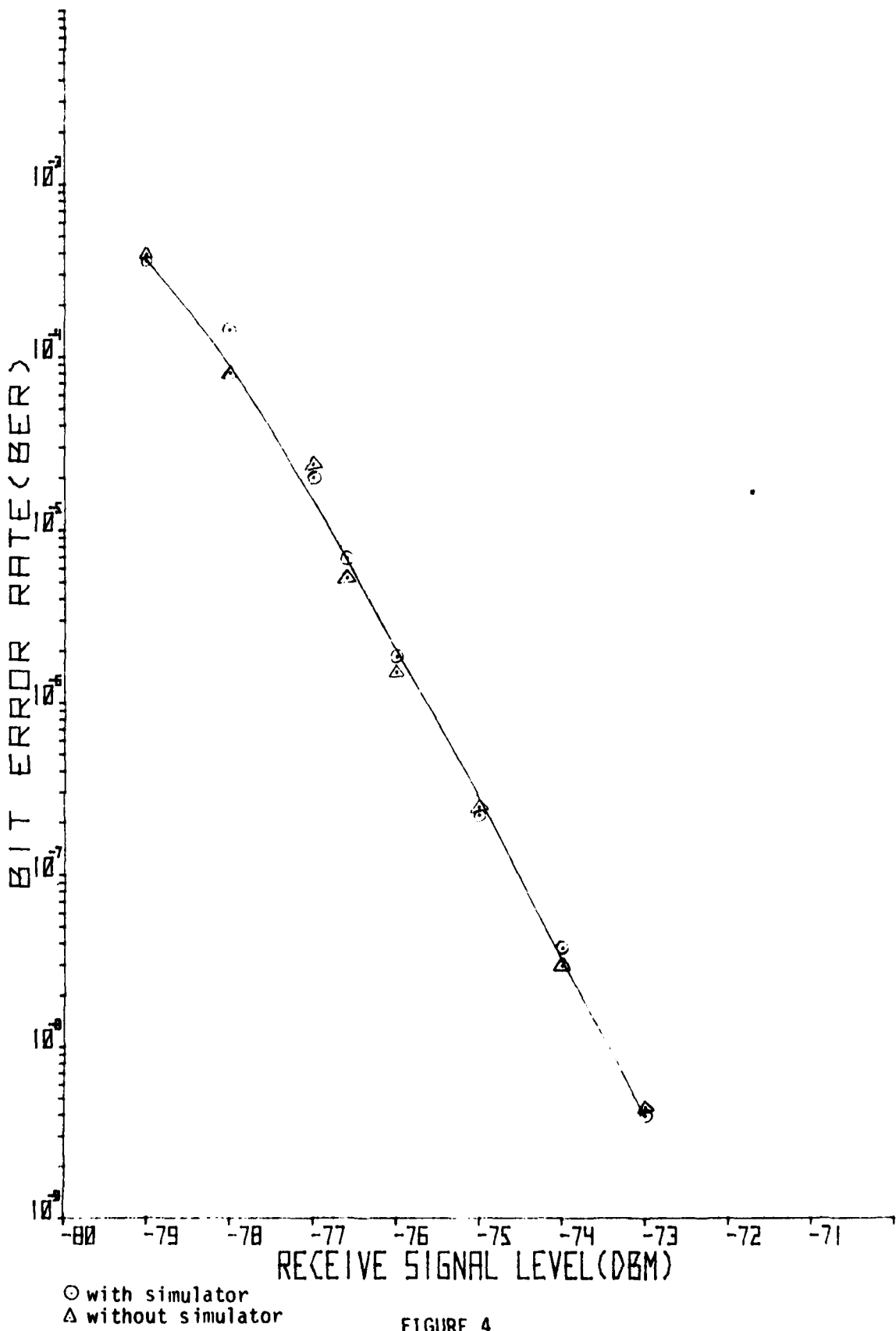


FIGURE 4

d. By varying the lower attenuator (item 7, figure 3) located between points (4) and (5), the notch depth (1-b) is adjusted so that several data points (readings of BER versus notch depth) are obtained in the BER range of  $10^{-8}$  to  $10^{-3}$ .

e. Step (d) is repeated for seven notch frequencies: 65.5 MHz, 67.5 MHz, 68.25 MHz, 70 MHz, 71.75 MHz, 73.5 MHz, and 74.5 MHz.

f. Steps (d) and (e) are repeated for three input RSL values (-30 dBm, -45 dBm, and -60 dBm) which effects changes in the value of the a parameter.

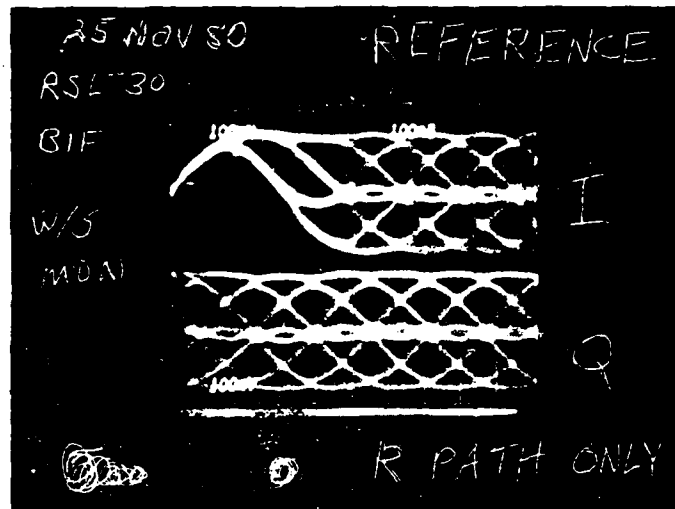
g. Steps (d), (e), (f), are repeated for four delay values (32 nsec, 16 nsec, 8 nsec, and 4 nsec).

### 3. RESULTS

#### 3.1 Qualitative.

3.1.1 Eye Pattern Closure: The eye pattern was monitored to obtain a qualitative description of signal degradation. Figures 6a and 7a corresponding to BER of  $6 \times 10^{-9}$  and  $7 \times 10^{-4}$  respectively, show considerable eye closure when contrasted with Figure 5a, corresponding to error free performance. As can be seen, however, the difference in eye closure in Figures 6 and 7 is not readily discernable even though the BER differs by several orders of magnitude. Since the purpose of monitoring the eye pattern was only to obtain a qualitative description of degradation, no attempt was made to improve the resolution of the eye pattern display.

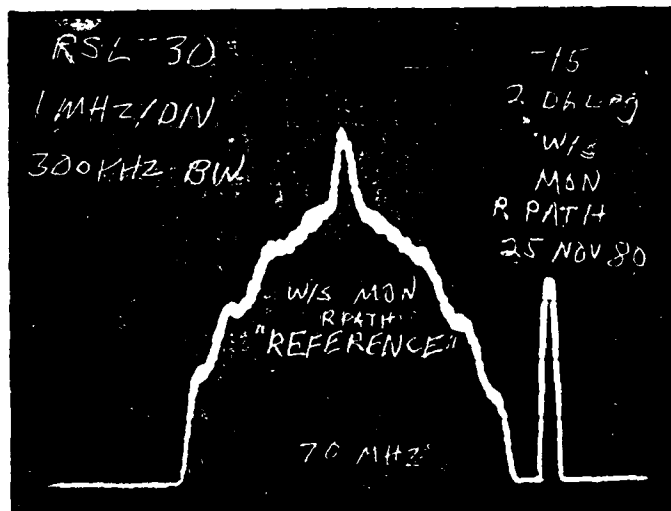
3.1.2 Spectrum Distortion: As with eye patterns, the radio IF spectrum was monitored to obtain a qualitative description of signal degradation. Figures 5b, 6b, and 7b are the corresponding IF spectrums for the eye patterns previously mentioned. Additionally, a spectrum with notch located in center



Remarks

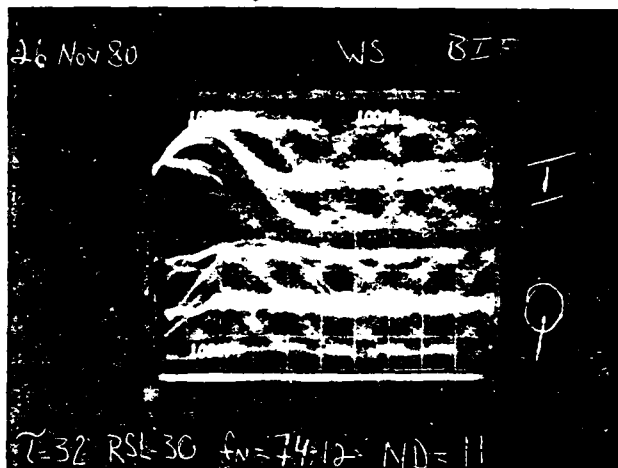
RECEIVE I and Q CHANNEL EYE PATTERN  
NO MULTIPATH, NO ERRORS OBSERVED

FIGURE 5a



Remarks RECEIVE SPECTRUM AT MONITOR POINT  
 R- PATH ONLY    RSL = -30 dBm    TIME DELAY = 0 nsec

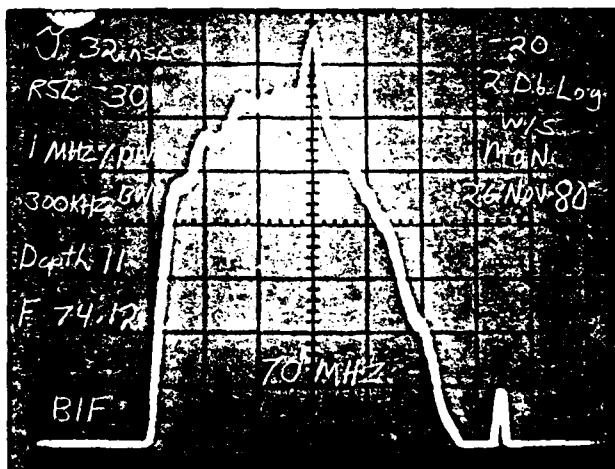
FIGURE 5b



Remarks

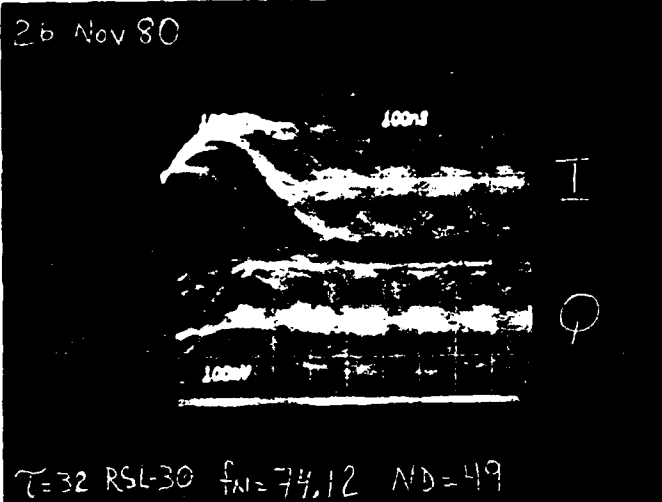
I and Q CHANNEL EYE PATTERN  
 $BER = 5.97 \times 10^{-9}$

FIGURE 6a



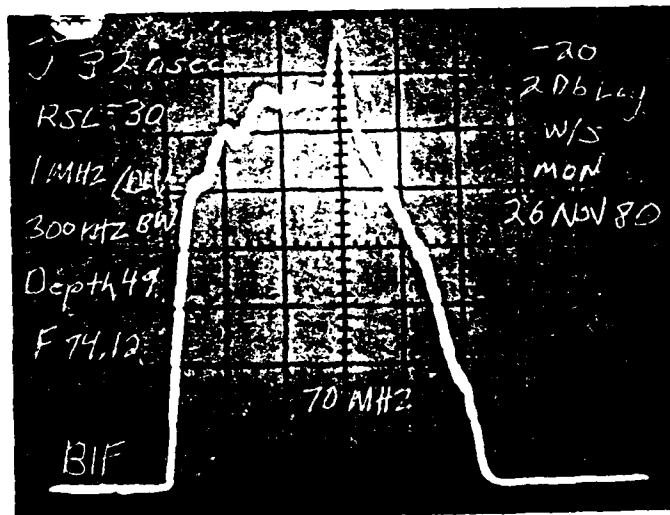
Remarks RECEIVE SPECTRUM, 32 nsec, RSL = -30 dB  
 NOTCH FREQUENCY = 74.12 MHz, NOTCH DEPTH = 11 dB

FIGURE 6b



Remarks  
I and Q CHANNEL EYE PATTERN  
 $\text{BER} = 7.61 \times 10^{-4}$

FIGURE 7a



Remarks RECEIVE SPECTRUM, 32 nsec, RSL = -30 dBm  
NOTCH FREQUENCY = 74.12 MHz, NOTCH DEPTH = 49 dB

FIGURE 7b

(70 MHz) is shown in Figure 8. The combination of the shape of the QPRS spectrum and the spectrum analyzer characteristics made it difficult to discern the location of the notch frequency and impossible to obtain the notch depth directly from the IF spectrum. The values of those parameters were obtained visually using a signal generator as the signal source.

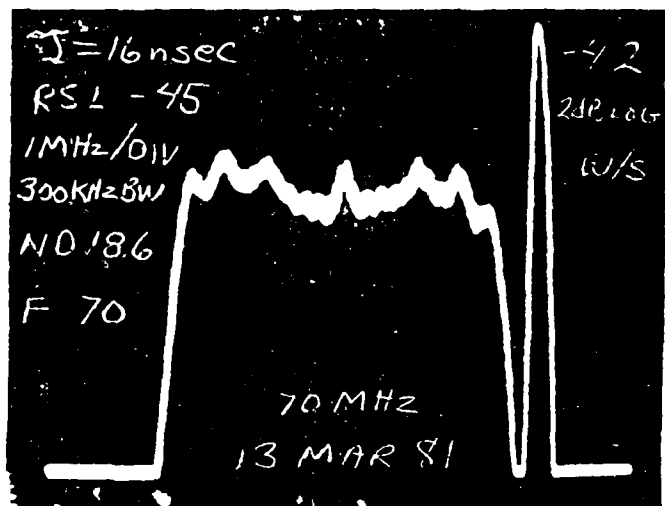
### 3.2 Quantitative.

3.2.1 Data Obtained: As described in Section 2.3, with each of the other parameters fixed, the notch depth was varied so that several points (BER values) are obtained for  $10^{-8} \leq \text{BER} \leq 10^{-3}$ . Typical curves are shown in Figures 9 through 12.

3.2.2 Received Signal Level Indication: The traditional method of monitoring signal quality is the received signal level as indicated by AGC voltage. However, if a link is experiencing frequency selective fading, the performance may be poorer than the RSL would normally indicate. The AGC voltage data indicates that for long delays, the actual drop in signal power is very small. Table 5 shows the drop in signal level as indicated by the AGC voltage for BER of  $10^{-4}$ . The notch frequency was  $\pm 3.5$  MHz from the band center.

TABLE 5

<u>Delay (nsec)</u>	<u>Notch Depth (dB)</u>	<u>Signal Level Drop (dB)</u>
4	27.4	19.8
8	19.3	14.5
16	13.9	8.5
32	9.3	3.3



Remarks: SIMULATOR OUTPUT:  $\tau = 16 \text{ nsec}$ , RSL = -45 dBm  
NOTCH DEPTH = 18.6 dB, NOTCH FREQUENCY = 70 MHz  
BER =  $5.67 \times 10^{-4}$

K-E SEMI-LOGARITHMIC 7 CYCLES X 60 DIVISIONS  
KEUFFEL & ESSEN CO MADE IN U.S.A.

46 6460

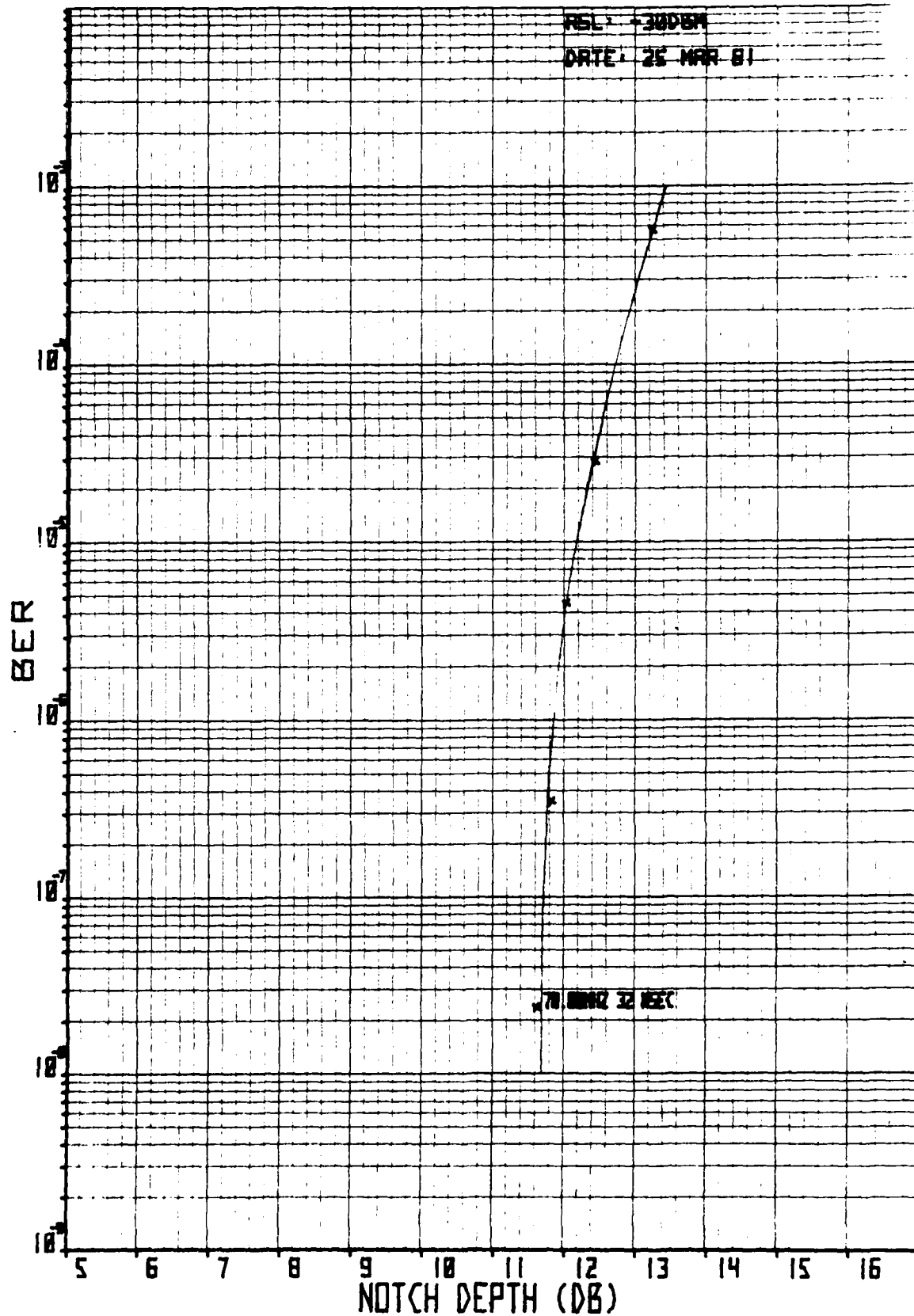


FIGURE 9

K-E SEMILOGARITHMIC 7 CYCLES X 60 DIVISIONS  
MADE IN U.S.A.  
KEUFFEL & ESSER CO.

46 6460

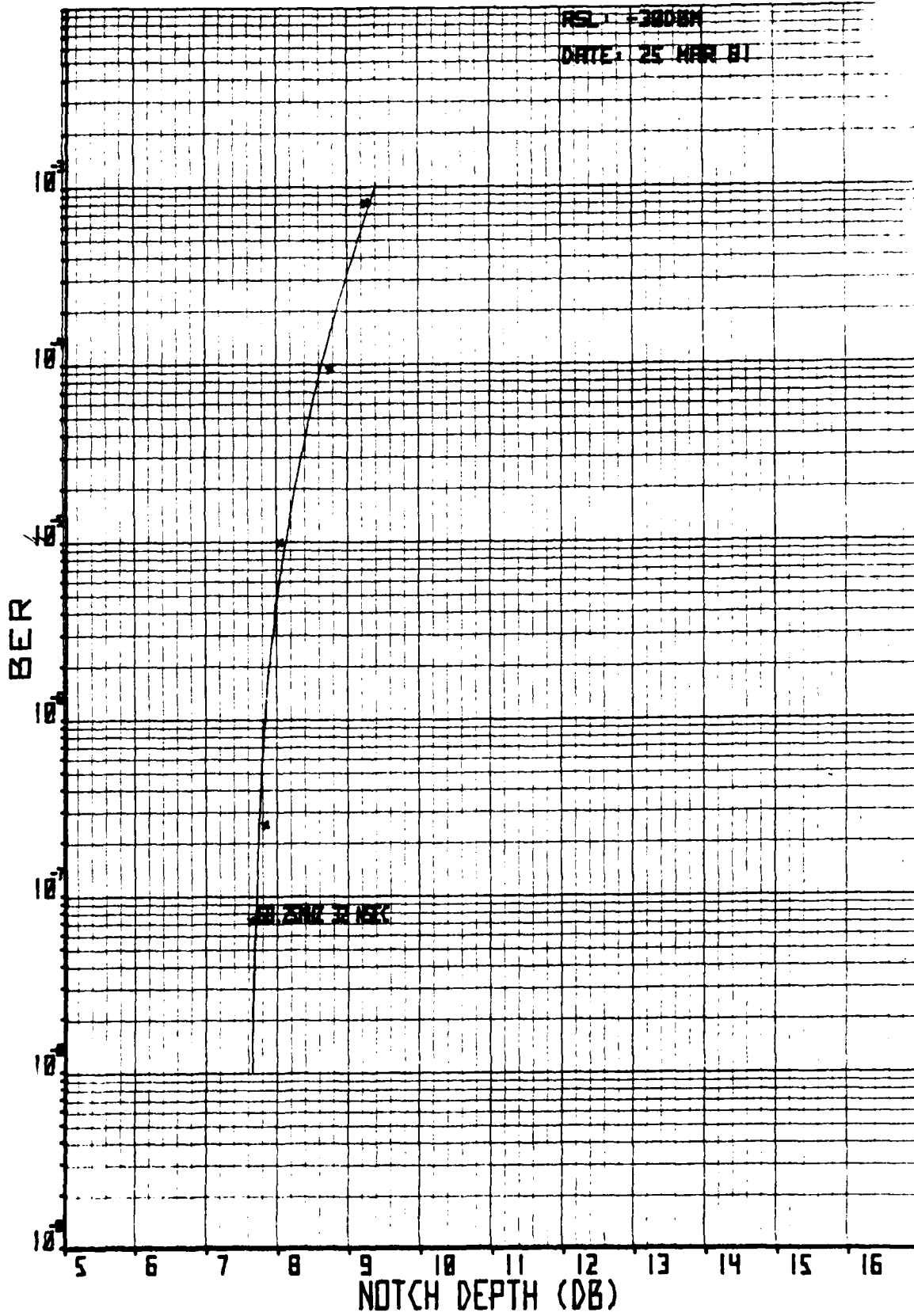


FIGURE 10

K-E SEMI-LOGARITHMIC 7 CYCLES X 60 DIVISIONS  
KENNELL & ESSER CO. MADE IN U.S.A.

46 6460

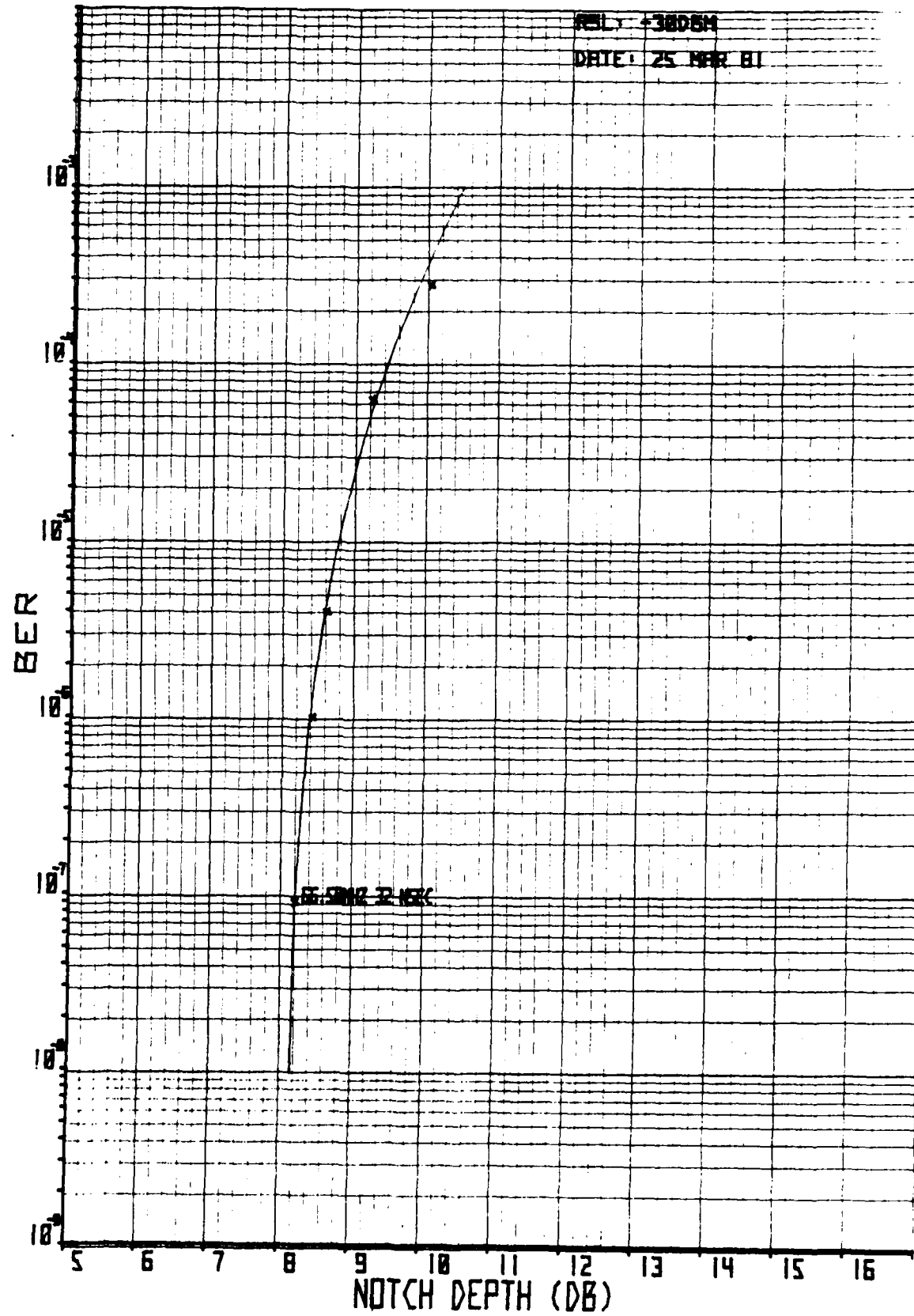


FIGURE 11  
20

K-E SEMI-LOGARITHMIC 7 CYCLES X 60 DIVISIONS  
KEUFFEL & ESSER CO. MADE IN U.S.A.

46 6460

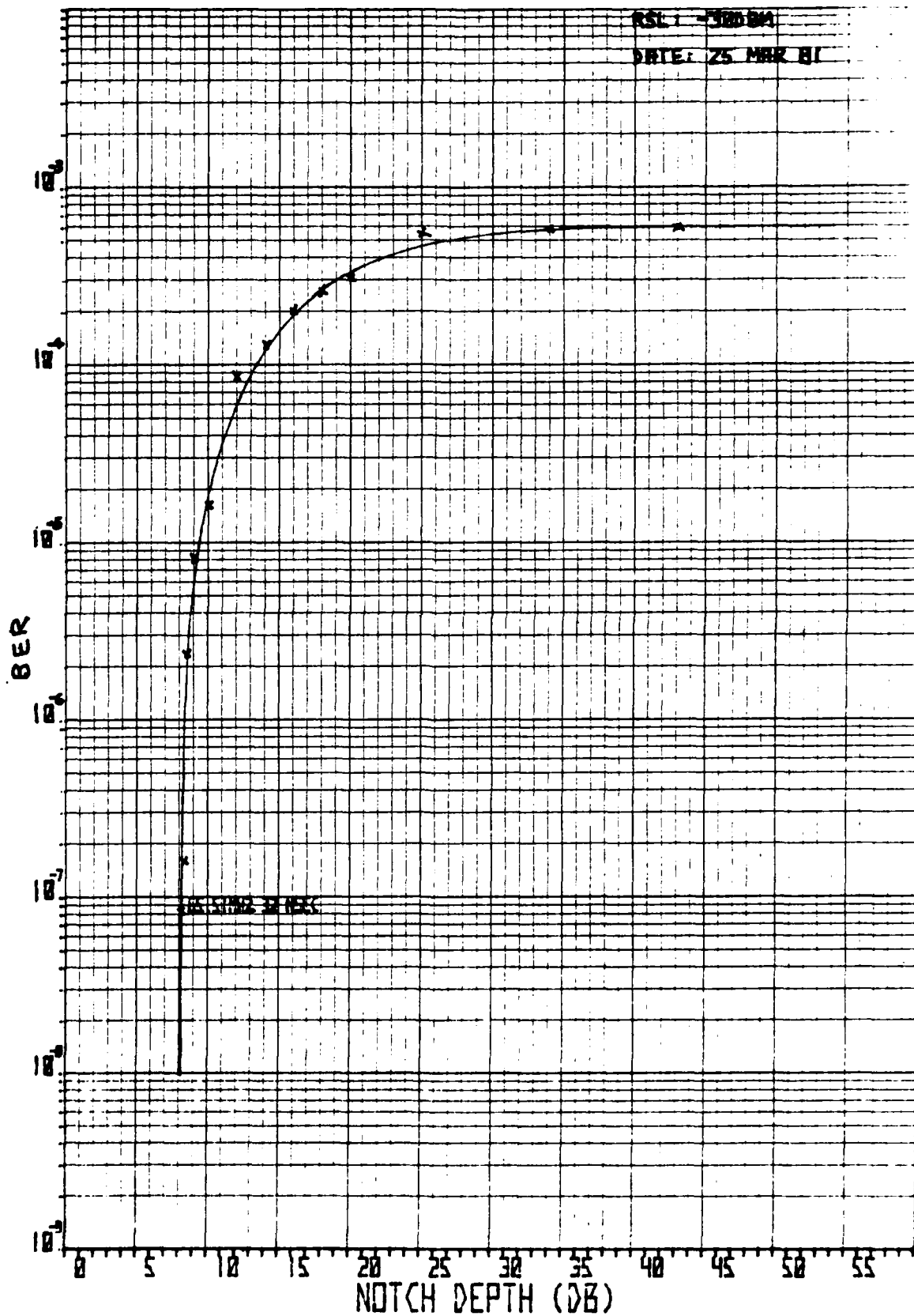


FIGURE 12

3.2.3 Critical Regions: If the value of the a parameter is fixed and the notch depth versus notch frequency is plotted for each value of delay, the result is Figure 13. As can be seen, the width of the critical region is essentially constant, and the height increases with increasing delay. Also, the critical region becomes larger in both width and height as the criteria for outage is changed to a lower BER as shown in Figure 14. Finally, there was no change in the critical region with change in values for the a parameter (within the values used). An illustration of this is shown in Figures 15 and 16 ( $BER = 10^{-4}$ ). Had the a parameter been decreased further however, there should have been an increase in the size of the critical region as reported by Emshwiller [5].

3.3 Outage Estimation. Having defined the critical regions for a given outage criterion, the amount of outage can be estimated if the statistics for the parameters of the channel transfer function are known. Unfortunately, there is insufficient data in this area and many assumptions must be made.

3.3.1 Determination of the Probability of Multipath Outage: The amount of outage caused by multipath is estimated by determining the probability of multipath outage:

$$P_m(\text{outage}) = P(b, \tau, \phi|M)P(M) \quad (2)$$

$$\text{where } P(b, \tau, \phi|M) = \iint_{\text{Critical Region}} P(b, \tau, \phi|M) db d\tau d\phi \quad (3)$$

$P(M)$  = Probability of multipath occurrence

and the critical region is the region where the BER is  $10^{-4}$  or greater. Proceeding in a similar fashion to [5], [6], [7], statistical independence is first assumed, allowing each of the random variable to be treated separately. Also since the a parameter did not affect the critical region, it

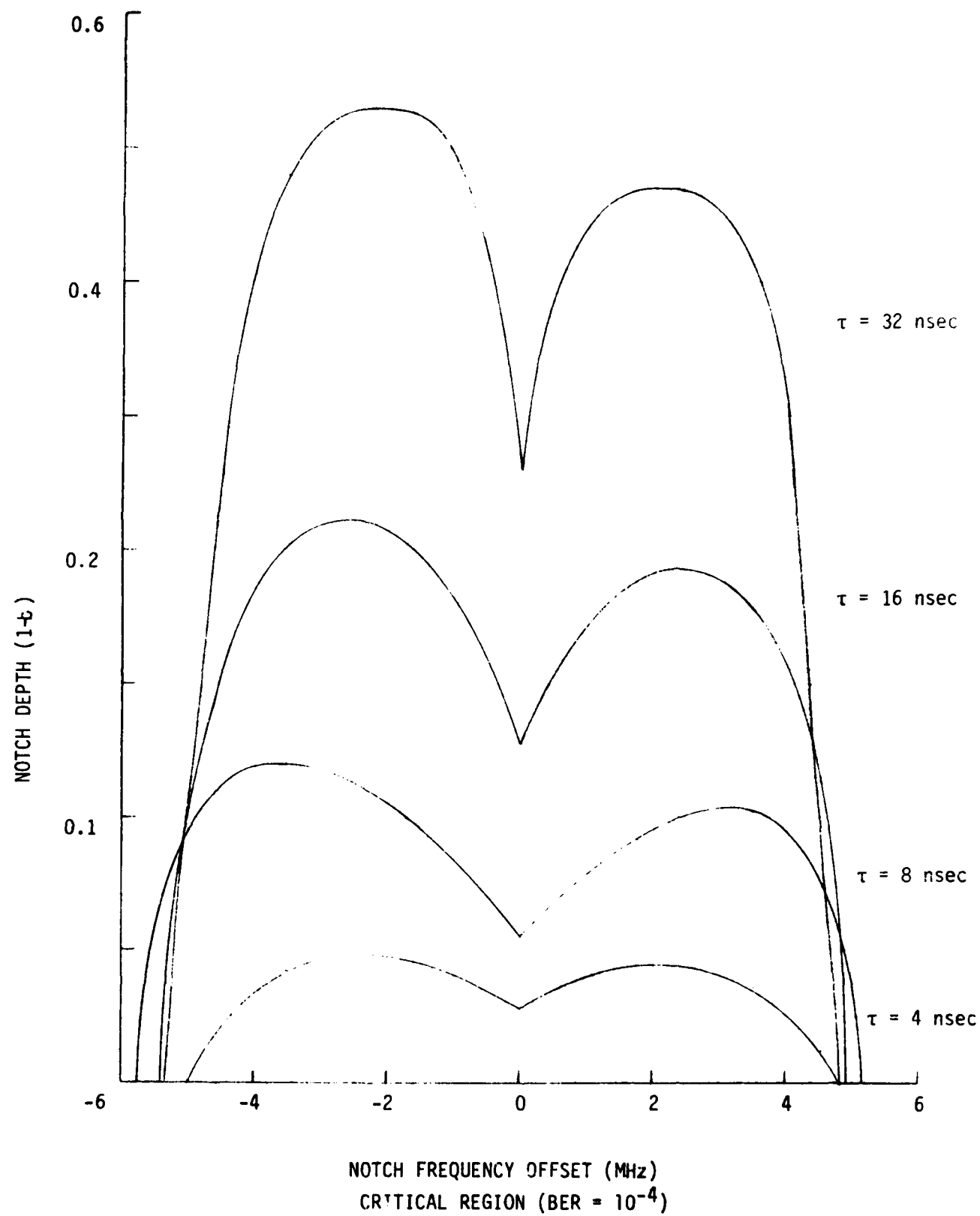
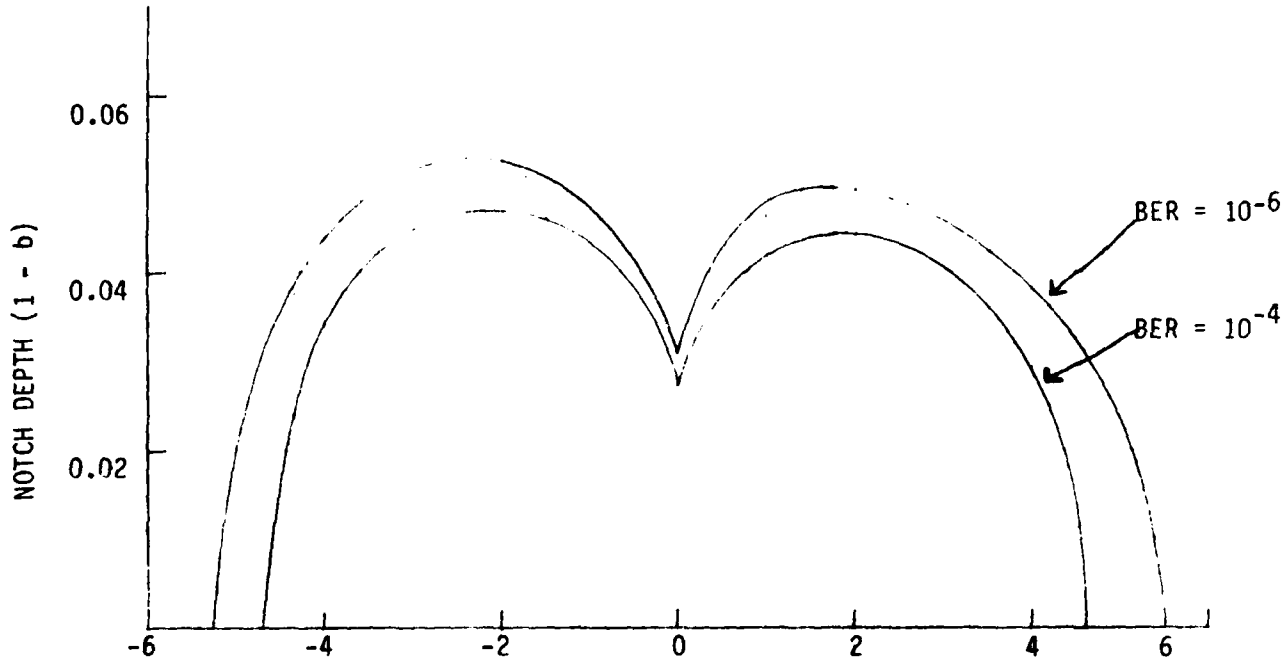
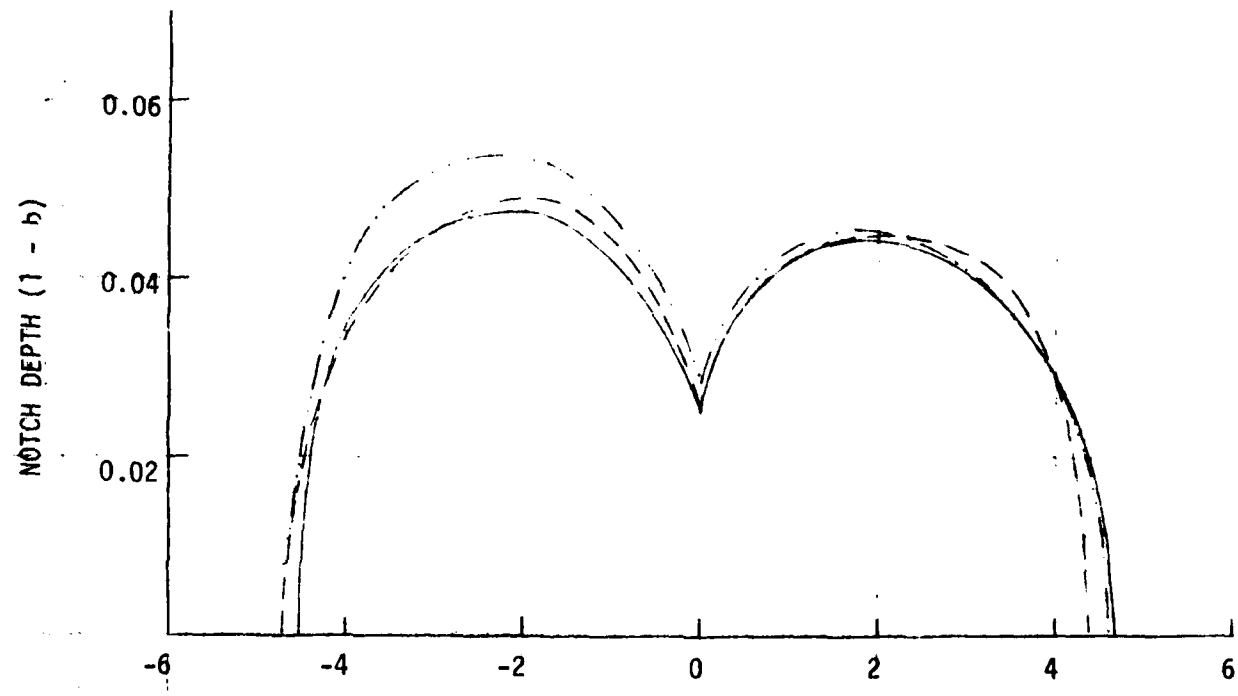


FIGURE 13



NOTCH FREQUENCY OFFSET (MHz)  
CRITICAL REGION FOR BER of  $10^{-4}$  and  $10^{-6}$  ( $\tau=4$  nsec)

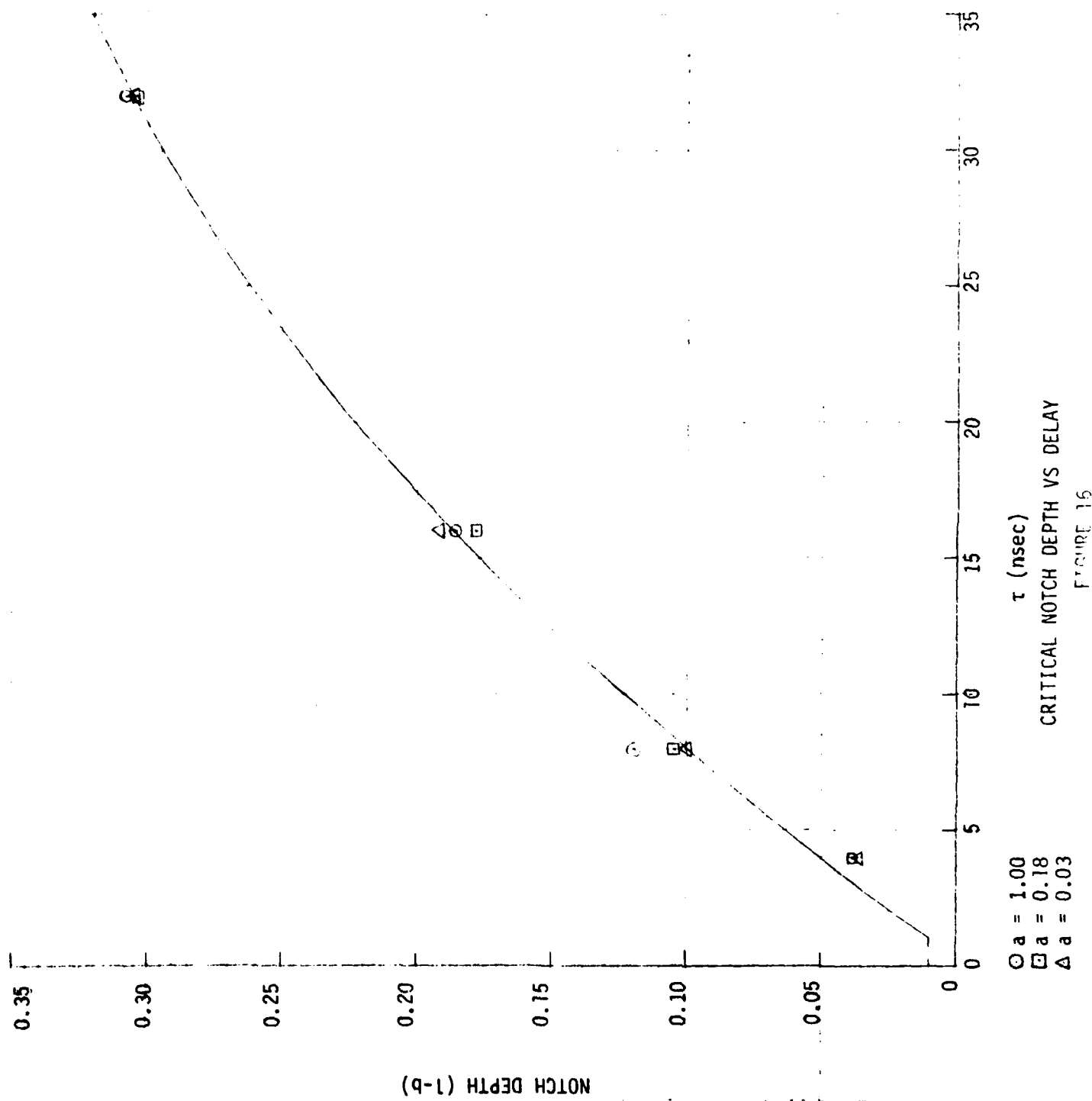
FIGURE 14



NOTCH FREQUENCY OFFSET (MHz)  
 CRITICAL REGION (BER =  $10^{-4}$ ,  $\tau = 4$  nsec)

- a = 1.0
- a = 0.18
- .. a = 0.03

FIGURE 15



NOTCH DEPTH ( $1-b$ )

$\circ \alpha = 1.00$   
 $\square \alpha = 0.18$   
 $\triangle \alpha = 0.03$   
 CRITICAL NOTCH DEPTH VS DELAY  
 FIGURE 16

is set to one. Having no reason to decide otherwise, a uniform distribution is assumed for the phase variable. The total critical width as fraction of the total width (width between notches) can then be expressed as:

$$P(\phi | \tau, M) = W\tau \leq 1 \quad (4)$$

where  $W$  = critical width.

A uniform distribution is also assumed for the ratio of amplitudes ( $b$  variable). This is based on CCIR Report 338-3 [8]. Having done this, the next step is to put the contour of the critical region into a usable form. Emshwiller [5] suggests converting the contour shown in Figure 13 into rectangles with the same area. For this study the width of the equivalent rectangle is at the one half height points. The average of those widths for all the contours (12 in all) is used as the equivalent critical width. Once the width is fixed, the critical height is just that height that satisfies the requirement that the area of the rectangle is equal to the area under the Figure 13 contour. This equivalent critical height is used for the  $(1-b)$  parameter. For the test radio, the equivalent width is 9.35 MHz with a standard deviation of 0.67 MHz, and a plot of the equivalent critical height  $(1-b)$  for  $\text{BER} = 10^{-4}$  versus delay  $(\tau)$  is shown in Figure 16. The quadratic:

$$x = (1-b) = C_0 + C_1\tau + C_2\tau^2 \quad (5)$$

where  $C_0 = -0.004154$

$$C_1 = 0.01417$$

$$C_2 = -0.0001394$$

provides a reasonable fit. Equation (5) is also the conditional distribution for  $x$ .

Jakes [6], and Greenstein and Prabhu [7], assumed for the probability density function for  $\tau$  an exponential:

$$p(\tau) = (1/\tau_0) \exp(-\tau/\tau_0) \quad (6)$$

$$\text{where } \tau = .2627 (D/20)^3 \quad (7)$$

and  $D$  = distance (miles)

They based their choice for expressions (6) and (7) on experimental data and the work of Ruthroff [9]. Equation (3) can now be expressed as:

$$\begin{aligned} P(b, \tau, \Phi | M) &= \int_{\tau_A}^{\tau_B} W\tau (.01)(1/\tau_0) \exp(-\tau/\tau_0) d\tau \\ &\quad + \int_{\tau_A}^{\tau_B} W\tau (C_0 + C_1\tau + C_2\tau^2)(1/\tau_0) \exp(-\tau/\tau_0) d\tau \\ &\quad + \int_{\tau_B}^{1/W} W\tau (C_0 + C_1\tau_B + C_2\tau_B^2)(1/\tau_0) \exp(-\tau/\tau_0) d\tau \\ &\quad + \int_{1/W}^{\infty} (C_0 + C_1\tau_B + C_2\tau_B^2)(1/\tau_0) \exp(-\tau/\tau_0) d\tau \end{aligned} \quad (8)$$

where  $\tau_A$  is the point at which the line defined by equation (5) intersects the horizontal line defined by the flat fade margin. For a 40 dB fade margin  $\tau_A \approx 1$  nsec. Also, there is a value  $\tau_B$ , where the line will curve back down. This occurs at 51 nsec for the test radio. Beyond this point, it is assumed that the required notch depth does not change with increasing delay for a given outage criteria. The last integral in equation (8) comes about because when  $\tau$  exceeds  $1/W$ , there will always be a notch in the critical region. Actually, for the distances considered, the last two terms are insignificant and can be ignored.

The final term to be developed in equation (2) is  $P(M)$ . This term is obtained from CCIR [8], which is based on the work of Morita [10]. The expression for a fading month is:

$$P(M) = KQf^B d^C \leq 1 \quad (9)$$

where  $d$  = path length (km)

$f$  = frequency (GHz)

$K$  = Climate factor =  $6 \times 10^{-7}$  (for continental US inland, non-mountainous region)

$Q$  = terrain factor = 1 (for average US terrain)

$B$  = 1 (for US)

$C$  = 3 (for US)

The resulting probability of outage is plotted for link distances to 50 miles in Figure 17 (unlabeled curve). For comparison purposes, also plotted are:

- Probability of outage assuming flat fades only (from CCIR [8]):

$$P(P_r) = KQ(P_r) f^B d^C \quad (10)$$

where  $P_r$  = ratio of faded to unfaded power (0.0001 used for 40 dB fade margin), and the other factors are identical to (9).

- Probability of outage using the method of Jakes [6] described below.

3.3.2 Determination of Jakes' k Factor: Jakes' formula to calculate outage is:

$$P_m(\text{outage}) = (1.6 R k^{0.85} / uv)(1+u/v) \quad (11)$$

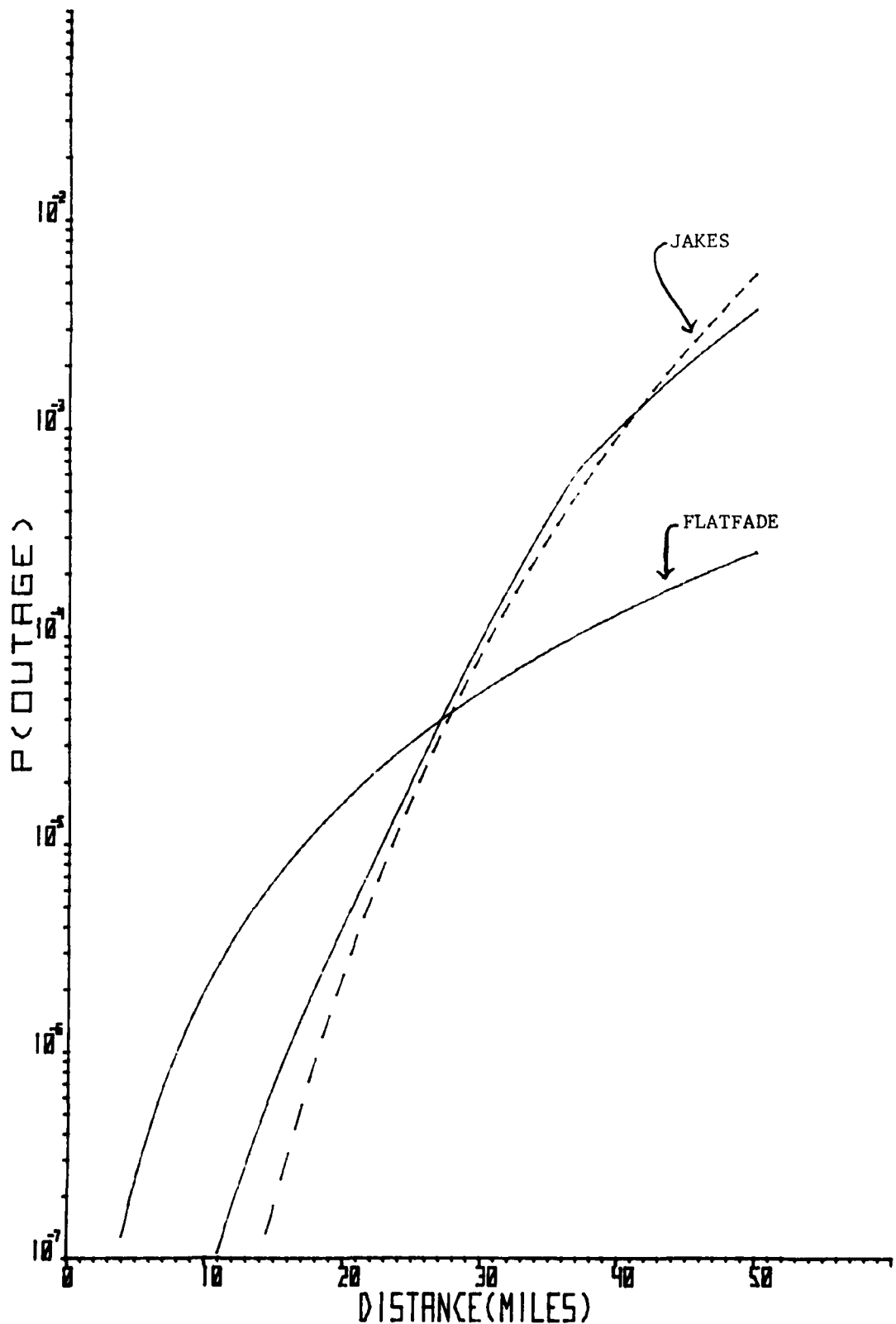
where  $R = 2.5 \times 10^{-6} CfD^3$

$C$  = climate factor = 1 (for average terrain)

$f$  = frequency (GHz)

$D$  = distance (miles)

$$u = (\tau_s / \tau_0) k^{0.85}$$



ESTIMATED OUTAGE

FIGURE 17

$$\tau_0 = .2627(D/20)^3 \text{ (as in equation (7))}$$

$$\tau_s = \text{symbol length} = 159 \text{ nsec (for DR-8A at } 12.5526 \text{ Mb/sec)}$$

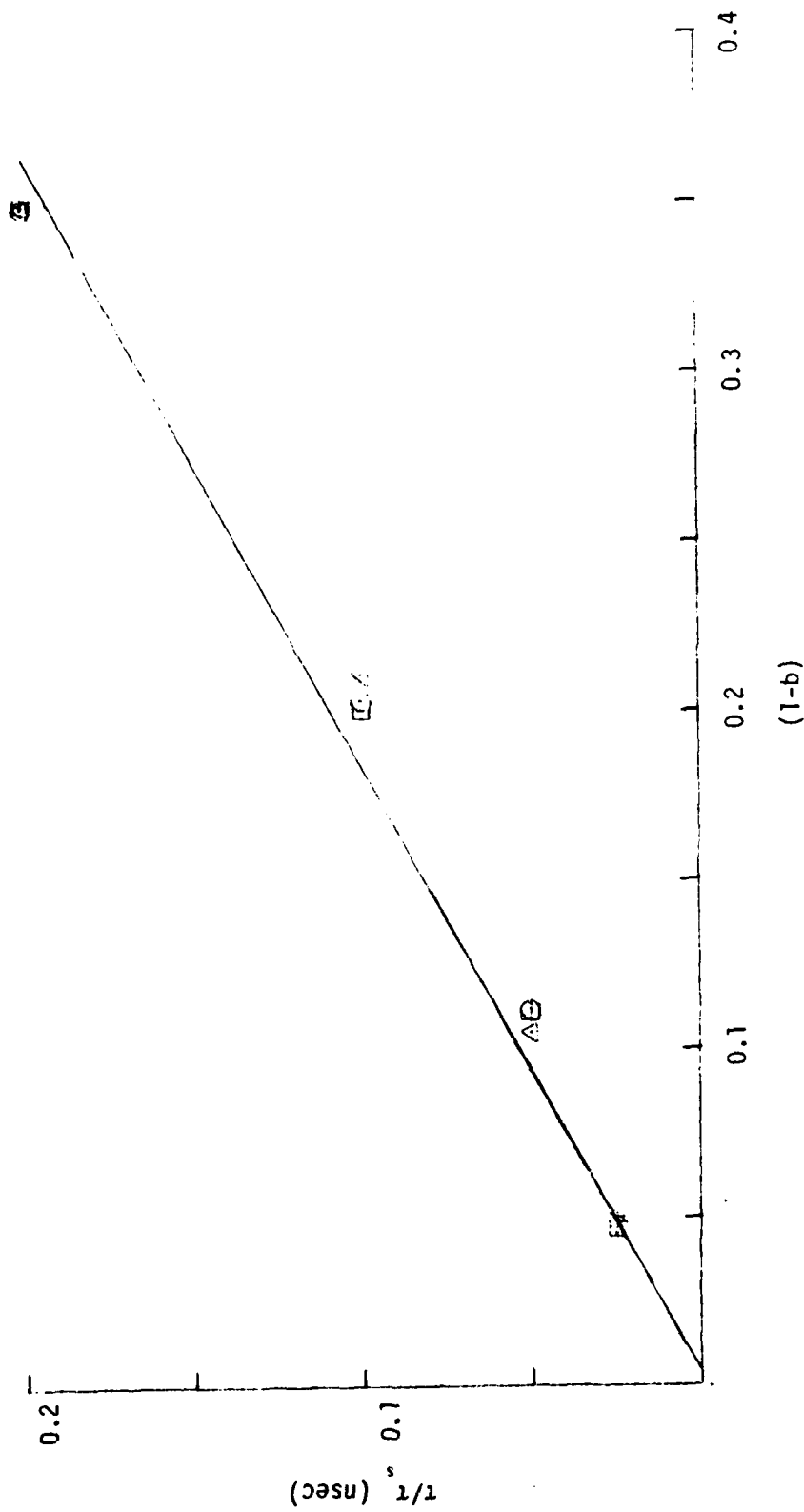
$$v = 10 + u$$

Jakes concludes that outage only occurs when the notch frequency is within 0.2xbandwidth of either band edge. The band edges ( $\pm 3.14$  MHz for 159 nsec) correspond approximately to the peaks in Figure 13. The only parameter that must be obtained from experimental data is the factor k, which occurs in the equation:

$$\tau_c = \tau_s^{k^{0.85}(1-b)} \quad (12)$$

If the average peaks in Figure 13 are used for (1-b) and are plotted against  $\tau_c/\tau_s$ , the result is Figure 18. The slope of the line in the figure is 0.56 and therefore k is 0.5. Jakes has determined that for QPSK, k = 0.7 and for 8PSK, k = 0.2, which places QPRS between the two.

3.3.3 Diversity Improvement: Anderson, et al [2], reported that for the 91 Mb/sec QPRS radio system employed by Bell Northern Research (BNR), a combining diversity system alone did not provide enough improvement to enable BNR to achieve their link performance objective. However, the addition of adaptive equalization did. The AN/FRC-171 employs a hitless switching space diversity system. The switch stimuli is to include signal quality as well as level. Giuffrida [11] compared the performance improvements of a switching diversity system, both with and without adaptive equalization, as well as a combining diversity system, with and without adaptive equalization on a link with frequency selective fading. Giuffrida reported that the switching diversity system improved link performance a factor of 12 and the combining



CRITICAL  $\tau_c/\tau_s$ , FOR A GIVEN NOTCH DEPTH

(1-b)  
FIGURE 18

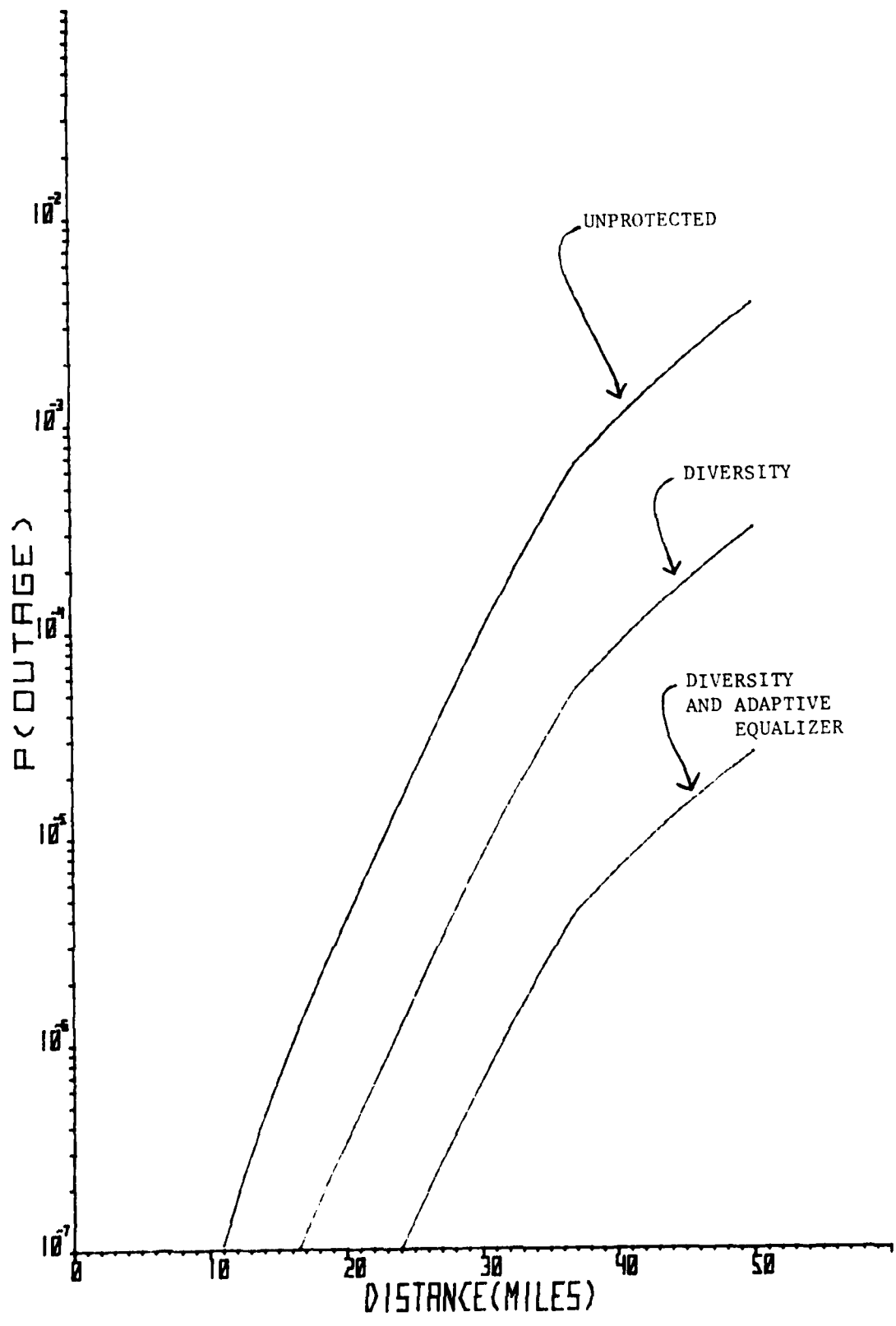
diversity system a factor of 6. The addition of adaptive equalization brought the total improvement to a factor of 145 and 175 respectively. Assuming the same improvement factors (12 and 145) and also assuming that these factors remain constant with distance the results are shown in Figure 19.

3.3.4 Media Unavailability Criterion: DCEC [12] specifies that the value  $3.5 \times 10^{-6}$  should be used as the "media unavailability criterion" for a nominal 30 mile link. If a three month fade reason is assumed then the value becomes  $1.4 \times 10^{-5}$  for a fading month. That point occurs slightly above the diversity line in Figure 19, implying that the criterion is satisfied (with a small margin) at that distance. However, it can also be seen that, due to the steepness of the curves in Figure 19, the criterion may not be satisfied with diversity along for distances slightly greater than 30 miles. Approximately 28 percent of the line-of-sight (LOS) links in the Defense Communications System exceed 30 miles in length (Parker [13]).

#### 4. CONCLUSIONS.

It is concluded that:

- a. The performance of the QPRS radio is degraded in a frequency selective fading environment.
- b. For distances exceeding 25 miles the outage for the unprotected digital radio link should be greater than that predicted assuming only flat fades.
- c. The performance of the QPRS radio in a frequency selective fading environment is nearly centered between QPSK (better) and 8PSK (worse).



ESTIMATED OUTAGE

FIGURE 19

d. Although there is a lack of experimental data to substantiate the results, they show that, depending on the data rate (and resulting bandwidth) and distance, dual diversity alone may not provide enough performance improvements for long links in regions with high multipath occurrence.

e. The combination of space diversity and adaptive equalizer such as used in the Bell Labs system [8] may be sufficient for nearly all LOS applications.

f. The method derived herein (and also in Jakes) underestimates the predicted outage for short paths (less than 25 miles).

g. Additional experimental work should be performed to eliminate the need for assumptions.

## 5. RECOMMENDATIONS.

It is recommended that:

a. The follow-on multipath simulation to be conducted on the AN/FRC-171 radio be performed with the following changes:

- (1) The variation of the  $\alpha$  parameter be eliminated.
- (2) The signal to noise ratio be varied for short delays (less than six nanoseconds) to better define the influence of thermal noise.

b. Digital radio link tests be conducted and the statistics for the parameters in the channel model be obtained.

c. Link testing be performed with the AN/FRC-171 on a link with high multipath occurrence, such as at the Pacific Missile Test Center.

#### REFERENCES

1. Rummier, W. D., "A New Selective Fading Model: Application to Propagation Data," Bell System Technical Journal, Vol. 58, No. 5, May-June 1979.
2. Anderson, C. W., S. Barber, and R. Patel, "The Effect of Selective Fading on Digital Radio," IEEE International Conference on Communication, Toronto, Ontario, June 1978.
3. Lundgren, C. W., and W. D. Rummier, "Digital Radio Outage Due to Selective Fading-Observation versus Prediction from Laboratory Simulation," Bell System Technical Journal, Vol. 58, No. 5, May-June 1979.
4. Lundgren, C. W., "A Methodology for Predicting Nondiversity Outage of High Capacity Digital Radio Systems," IEEE International Conference on Communications, Boston, MA, June 1979.
5. Emshwiller, M., "Characterization of the Performance of PSK Digital Radio Transmission in the Presence of Multipath Fading," IEEE International Conference on Communications, Toronto, Ontario, June 1978.
6. Jakes, W. C., Jr., "An Approximate Method to Estimate an Upper Bound on the Effect of Multipath Delay Distortion on Digital Transmission," IEEE Transactions on Communications, Vol. Comm-27, No. 1, January 1979.
7. Greenstein, L. J. and V. K. Prabhu, "Analysis of Multipath Outage with Applications to 90 Mbit/sec PSK Systems at 6 and 11 GHz," IEEE Transactions on Communications, Vol. Comm-27, No. 1, January 1979.
8. CCIR, Report 338-3, "Propagation Data Required for Line-of-Sight Radio Relay Systems," Vol. 5, 1978.

9. Ruthroff, C. L., "Multipath Fading on Line-of-Sight Microwave Radio Systems as a Function of Path Length and Frequency," Bell System Technical Journal, Vol. 50, No. 7, September 1971.
10. Morita, K., "Prediction of Rayleigh Fading Occurrence Probability of Line-of-Sight Microwave Links," Review of the Electrical Communications Laboratory, Vol. 18, No. 11-12, Nov-Dec 1970.
11. Giuffrida, T. S., "Measurements of the Effects of Propagation on Digital Radio Systems Equipped with Space Diversity and Adaptive Equalization," IEEE International Conference on Communications, Boston, MA, June 1979.
12. Kirk, K. W. and J. L. Osterholz, "DCS Digital Transmission System Performance," Defense Communications Engineering Center Technical Report No. 12-76, November 1976.
13. Parker, D. E., "Design Objectives for DCS LOS Digital Radio Links", Defense Communications Engineering Center Engineering Publication No. 27-77, December 1977.

## APPENDIX

### IF SIMULATION

Hardware constraints make it apparent that the fade simulation is better performed at IF rather than at RF even though the transfer function to be simulated occurs at RF. As seen below, with the proper phase adjustment (modulo  $2\pi$ ) the IF simulation can be made identical to the RF simulation

At RF the resulting signal is:

$$G_{RF}(\omega) = F_{RF}(\omega)H_{RF}(\omega)$$

where  $F_{RF}(\omega)$  = transmitted RF signal

$$H_{RF}(\omega) = a\{1+b\exp[-j(\omega\tau+\phi)]\}$$

let  $\omega = \omega_c \pm \omega_i$

where  $\omega_c$  = carrier radian frequency

$\omega_i$  = baseband frequency component

$$\text{Therefore, } H_{RF}(\omega) = a\{1+b\exp[-j(\pm\omega_i\tau+\omega_c\tau+\phi)]\}$$

It can be shown that after down converting,

$$G_{IF}(\omega) = F_{IF}(\omega)H_{RF}(\omega)$$

where  $F_{IF}(\omega) = KF_{RF}(\omega_{IF} \pm \omega_i)$

However the IF fade simulator results in

$$G_{IF}^1(\omega) = F_{IF}(\omega)H_{IF}(\omega)$$

where  $H_{IF}(\omega) = a\{1+b\exp[-j(\pm\omega_i\tau+\omega_{IF}\tau+\phi_{IF})]\}$

so that  $G_{IF}^1(\omega) = G_{IF}(\omega)$ ,

require that  $H_{IF}(\omega) = H_{RF}(\omega)$

and  $\omega_{IF}\tau + \phi_{IF} = \omega_c\tau + \phi$

or  $\phi_{IF} = (\omega_c - \omega_{IF})\tau + \phi$